

Features of supercooled glycerol dynamics

Ya. E. Ryabov,* Y. Hayashi, A. Gutina, and Y. Feldman†

Department of Applied Physics, School of Applied Science, The Hebrew University of Jerusalem, Givat Ram, 91904 Jerusalem, Israel

(Received 11 October 2002; published 11 April 2003)

In this work we compare the relaxation properties of pure dehydrated glycerol with those of the glycerol usually studied (the glycerol sample which is not specially protected from water absorption). We show that the dielectric spectroscopy can distinguish between the different structures and dynamics of these two kinds of glycerol. We report a relaxation dynamic in the pure dehydrated glycerol crystalline phase. We also show that the crystallization of the pure dehydrated glycerol near 263 K is accompanied by a specific process, which is observed in glycerol without a crystalline phase, by differential scanning calorimetry.

DOI: 10.1103/PhysRevB.67.132202

PACS number(s): 64.70.Pf, 65.60.+a, 77.22.Gm

The associated liquids as a group exhibit extremely rich dynamics and have a special place among many other glass formers.^{1–5} In particular, glycerol ($C_3H_8O_3$) has been widely used as a model system in many studies, both old⁶ and more recent^{7–19} of glassy substances and supercooled liquids. Usually glycerol exists only in a liquid, supercooled, or glassy state. However, after special treatment pure dehydrated glycerol can be crystallized.^{20,21} The un-crystallized glycerol is a common system used for studying glass-forming dynamics^{1–19} while crystallized glycerol, until now, has not been investigated.

Under normal conditions glycerol does not undergo crystallization but rather during cooling it becomes a supercooled liquid, which can be vitrified^{1,2,5,7,8,14} at $T_g = 190$ K. In contrast, anhydrous glycerol, cooled down below the glass-transition point T_g and then slowly heated up, can be crystallized.^{20,21} A well-known x-ray study²¹ of the glycerol structure employed more or less the same procedure of glycerol crystallization. However, the crystallization of glycerol is a very unusual and unstable process, which depends on the temperature history and impurities of the sample.

In our work we have made an attempt to investigate the main features of glycerol crystallization by comparison between the glass-forming dynamics of anhydrous glycerol and the glycerol that was not specially treated to prevent water absorption.

We used glycerol purchased from Fluka (Glycerine Analytical 5551900, assay by volume not less than 99.5%, H_2O content not more than 0.1%). The bottle of this glycerol was opened and then stored in desiccated nitrogen atmosphere at room temperature. From this glycerol we prepared two kinds of samples *A* and *B*.

To prevent water absorption for sample *A* all of the manipulations with this sample, such as filling of sample cells for dielectric spectroscopy and differential scanning calorimetry measurements, were performed in desiccated nitrogen atmosphere. Then the sample cells were hermetically sealed. Thus, we claim that for sample *A*, the water content remains the same as provided by the supplier. For sample *B* we did not take special care to prevent water absorption. The bottle of this glycerol was used and stored (closed with standard cap sealed with Parafilm tape) in regular laboratory conditions at normal pressure, room temperature 25 °C and relative humidity 35%. All the manipulations with this sample

were performed in the same conditions. For this sample we were not able to control water content, but, definitely the conditions of sample *B* preparation could be regarded as standard conditions for physical experiments.

To reach crystallization, we cooled sample *A* from room temperature to 133 K. Then measurements of the complex dielectric permittivity $\epsilon(f)$ against frequency f and temperature were performed by a Novocontrol Broadband Dielectric Spectroscopy 80 setup in the frequency interval from 0.01 Hz up to 3 MHz and for the temperature range from 133 K up to 325 K (see Fig. 1). Thus, overall experimental time was 30 h and average heating rate was about 0.1 K min⁻¹.

Considerable changes in $\epsilon(f)$ behavior in the measured frequency range are observed in the temperature interval from 263 K to 293 K. The transition at 293 K is known as

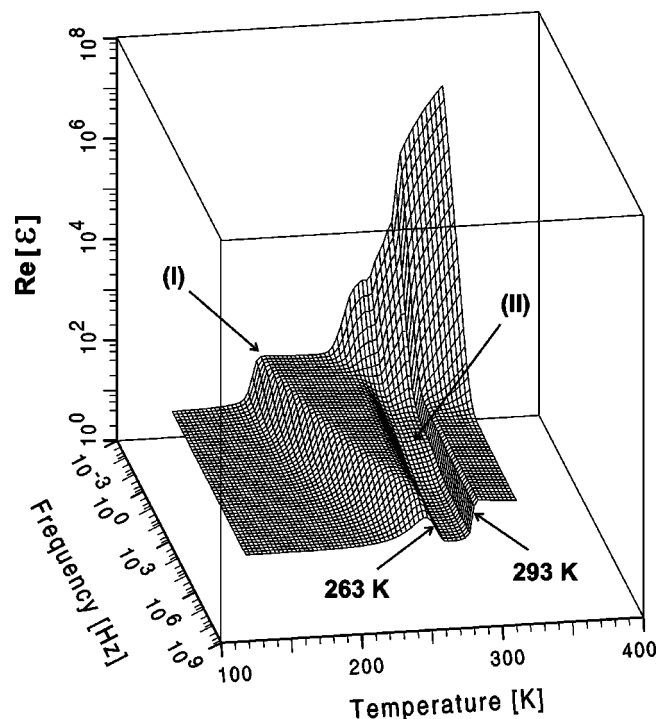


FIG. 1. A three-dimensional plot representing the real part of $\epsilon(f)$ for sample *A*. The arrows mark the crystallization temperature ($T_x = 263$ K), the melting point ($T_m = 293$ K), and the principal relaxation process, before (I) and after (II) the crystallization.

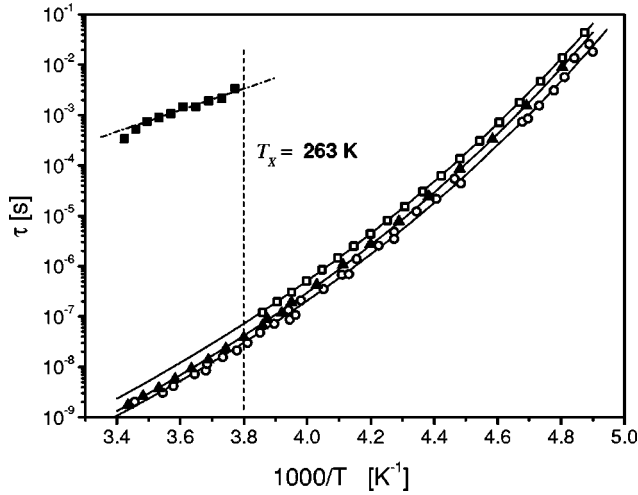


FIG. 2. Sample A before (open boxes) and after (full boxes) the crystallization compared with sample B (triangles), and literature data¹⁹ (circles). In the supercooled phase all samples obey a VFT law (full lines), while the relaxation process in sample A above 263 K obeys an Arrhenius law (dash-dotted line).

the glycerol melting point.²² Thus, the transition near 263 K is thought to be attributed to the glycerol crystallization. Note that the relaxation process (I) of the supercooled glycerol in this temperature interval disappears and the relaxation process (II), with a reduced strength, appears in the low-frequency region.

The data presented in Fig. 1 were analyzed as a set of isothermal spectra using the so-called Havriliak-Negami²³ empirical dependency

$$\varepsilon(f) = \varepsilon_{\infty} + \frac{\varepsilon_s - \varepsilon_{\infty}}{[1 + (i2\pi f\tau)^{\alpha}]^{\beta}}, \quad (1)$$

where τ is the relaxation time, ε_s and ε_{∞} are the low- and high-frequency limits of dielectric permittivity, and α and β are exponents reflecting symmetrical and unsymmetrical broadening of the relaxation peak. It is remarkable that in the liquid and supercooled phases, glycerol exhibits asymmetrical relaxation peak broadening ($\alpha \approx 1, \beta \approx 0.6$) whereas in the crystalline phase the broadening is rather symmetric ($0.6 \leq \alpha \leq 0.7, \beta = 1$).

To obtain the reference data we measured sample B in the usual way with a Novocontrol BDS 80 setup in the frequency interval from 2 Hz up to 1.8 MHz for the temperature range from 173 K up to 323 K. In this case, glycerol demonstrated an observed early dielectric response.¹⁻¹⁹ In Fig. 2, we compared temperature dependencies of fitted relaxation time for samples A and B and data recently published by Lunkenheimer and Loidl.¹⁹ The fitting yields that the process (I) in the supercooled phase for sample A, the relaxation in sample B, and literature data,¹⁹ all obey the Vogel-Fulcher-Tammann (VFT) law $\tau = \tau_v \exp[DT_v/(T - T_v)]$. From the data presented in Fig. 2 one can see that values of the VFT temperature T_v and fragility D are very close for all the samples where $D = 22 \pm 2$ and $T_v = 122 \pm 2$ K, while the preexponential factors τ_v are remarkably different. For the anhydrous

sample A $\tau_v = 3.9 \times 10^{-16}$ s, for sample B $\tau_v = 2.3 \times 10^{-16}$ s, while for the literature data¹⁹ $\tau_v = 1.7 \times 10^{-16}$ s. Taking into account the fact that sample A was specially protected from water absorption, it is strongly suspected that this big difference in τ_v is provided by water absorbed from the atmosphere. This observation signifies that even a very small water content can result in significantly different dynamics in the supercooled phase for the anhydrous glycerol and for the glycerol samples usually studied.¹⁻¹⁹

For the II relaxation process in sample A above 263 K, we observed the Arrhenius dependence of the dielectric relaxation time $\tau = \tau_0 \exp(E_a/kT)$ with an activation energy $E_a = 41 \pm 6$ kJ mol⁻¹ and $\tau_0 = 2.7 \times 10^{-11}$ s (see Fig. 2). The VFT behavior of supercooled glycerol is well known and noticed in many early works¹⁻¹⁹ while the Arrhenius relaxation is more relevant for crystals. For example, the temperature dependence of dielectric relaxation time of ice I also obeys²⁴⁻²⁶ an Arrhenius law with an activation energy of about 60 kJ mol⁻¹. It is known^{25,26} that the relaxation in ice I caused by the mobility of defects in the crystalline structure is provided either by the impurities or by the amorphous boundary layers between the crystallites. Therefore, the observed process II is most probably related to the crystalline phase of glycerol and caused by the mobility of defects in the crystalline lattice while process I could be related to a cooperative dynamics of glycerol in a supercooled phase.

The observed dynamical changes in anhydrous glycerol have to be accompanied by changes in mutual orientations of neighboring glycerol molecules. Let us further analyze the so-called Kirkwood correlation factor g , defined as $g = 1 + z \langle \cos \theta_{ij} \rangle$, where z is the number of nearest dipole neighbors and $\langle \cos \theta_{ij} \rangle$ is an averaged cosine of the angle θ_{ij} between two neighboring dipoles (see Ref. 27, and references therein). Thus, $g > 1$ signifies that the dipoles have a tendency for parallel orientation, $0 < g < 1$ implies antiparallel orientation while $g = 1$ corresponds to random dipole orientation. The Kirkwood correlation factor can be calculated using the following Kirkwood-Frlich formula:²⁷

$$g = \frac{9 \varepsilon_0 M k T (\varepsilon_s - \varepsilon_{\infty})(2\varepsilon_s + \varepsilon_{\infty})}{\rho N_a \mu^2 \varepsilon_s (\varepsilon_{\infty} + 2)^2}, \quad (2)$$

where $k = 1.381 \times 10^{-23}$ J K⁻¹ is the Boltzmann factor, $\varepsilon_0 = 8.854 \times 10^{-12}$ F m⁻¹ is the dielectric permittivity of free space, $N_a = 6.022 \times 10^{23}$ mol⁻¹ is the Avogadro's constant, $M = 0.921$ kg mol⁻¹ is the glycerol molar mass,²² $\mu = 8.91 \times 10^{-30}$ C m (2.67 D units) is the dipole moment of a glycerol molecule,²⁸ and ρ is the glycerol density. In the liquid²² phase of glycerol $\rho = 1261$ kg m⁻³ while in the crystalline²¹ phase $\rho = 1390$ kg m⁻³. The Kirkwood correlation factor calculated with Eq. (2) shows significant changes in g at 263 K for anhydrous glycerol (sample A), as presented in Fig. 3. In the room-temperature region, these estimations are in good agreement with early calculations⁶ of g . This behavior indicates the structural transition in the sample related to glycerol crystallization. Note that in the supercooled liquid phase of sample A before crystallization, the temperature dependence of parameter g is almost negligible, while for

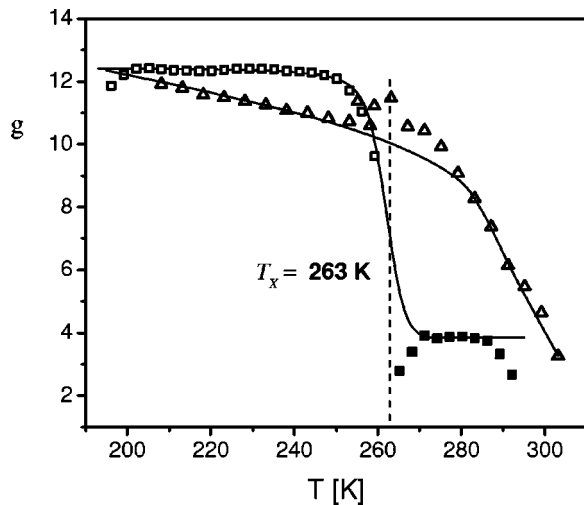


FIG. 3. The temperature dependence of the g , the Kirkwood correlation factor. Open boxes correspond to the relaxation process I in sample A. Full boxes correspond to the relaxation process II in sample A, while triangles correspond to the sample B. Values of ε_s and ε_∞ for g calculation were fitted with Eq. (1).

sample B behavior, without crystallization, it has a strong temperature dependence (see Fig. 3). This indicates that the two different dynamical patterns of glycerol behavior are related to two different structural organizations of glycerol in the supercooled liquid phase.

In addition to dielectric spectroscopy (DS) experiments, we performed differential scanning calorimetry (DSC) measurements of anhydrous sample A using a Mettler DSC-30 setup for the temperature interval from 133 K up to 303 K (see Fig. 4). As one can see in Fig. 4, there is no evidence of either crystallization or melting of the glycerol sample. In this regard one should note that the temperature treatments of the glycerol samples were different for the DS and DSC experiments. The average temperature increase rate in the

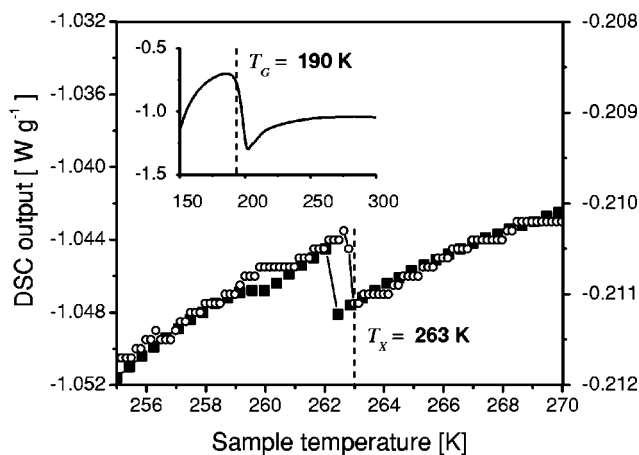


FIG. 4. DSC output heat flow for anhydrous sample A as a function of the sample temperature. The main window shows in detail the region of 263 K. Full boxes and left axis correspond to 25 K min^{-1} heating rate. Open circles and right axis correspond to 5 K min^{-1} heating rate. The inset window demonstrates the overall DSC signal for the experiment with a heating rate of 25 K min^{-1} .

DS experiment was 0.1 K min^{-1} . Regrettably, since the strength of the DSC output is in direct proportion to the heating rate, at 0.1 K min^{-1} relevant changes in signal were smaller than the precision of our DSC measurements. Thus, we used the standard 5 K min^{-1} and 25 K min^{-1} heating rates and the longest experiment presented in Fig. 4 has an overall time of 35 min. This heating rate is too fast to crystallize glycerol. However, detailed analysis shows some changes in the sample heat capacity at 263 K.

For further discussion, note that the dynamics of the glass-forming substances in supercooled and glassy states are usually characterized by several specific temperatures: the calorimetric glass-transition temperature T_g ; the critical temperature T_c of the idealized mode coupling theory²⁹ (MCT); the second scaling temperature T_x introduced¹³ to collapse all the curves in a viscosity fragility plot to a single universal VFT dependence, and others.^{3-5,9,30} Historically,¹³ the temperature T_x was introduced as an estimation of T_c from the viscosity fragility plot of a glass former. Later^{5,16} it was distinguished from the idealized MCT temperature T_c . Thus, for most glass-forming substances^{1-5,9,11,16} $T_c \sim (1.2-1.4)T_g$ and T_x is close to T_c . For glycerol^{1,2,5,7,8,14,22} $T_g = 190 \text{ K}$, T_c has been evaluated¹² at 262 K and T_x has been estimated¹³ at 259 K. At the same time, an attentive analysis of the experimental findings³¹⁻³⁶ leads to the conclusion that for many glass formers the crystallization rate reaches a maximum in the region of $(1.2-1.4)T_g$ (in other words near T_c). Our observation is that slowly heated, pure dehydrated glycerol starts to crystallize near 263 K, in fair agreement with estimations^{12,13} of glycerol, T_c and T_x . Therefore, at sufficiently low heating rates (about 0.1 K min^{-1}), crystallization occurs near T_c , since the crystallization rate reaches a maximum at this point. For faster (say 5 or 25 K min^{-1}) heating rates, even the fastest crystallization rate at T_c cannot provide glycerol crystallization.

The peculiarity of the DSC signal observed at 263 K is a subject of special interest. From one point of view this distinction could be considered as a sign of the crystallization onset that we observed in DS experiments. However, from Fig. 4 one can conclude that this feature seems to be endothermic or at least shaped like a glass-transition DSC fingerprint. In this regard, recall the discussion, which took place in the late 1970s of the last century.^{37,38} At that time Axelson and Mandelkern³⁷ analyzed experiential nuclear-magnetic-resonance (NMR) data of C^{13} relaxation for several glass-forming substances and found that C^{13} NMR spectra for all analyzed samples collapse at the T_{col} temperature well above the T_g observed by other experimental techniques. They discussed this temperature as an upper limit for the glass transition. Later Boyer and Gillham³⁸ suggested a different interpretation for T_{col} as another second-order liquid-liquid transition in the supercooled liquid state. Our observation of a DSC signal in the vicinity of 263 K is in fair agreement³⁷ with the $T_{col} = 267 \text{ K}$ mentioned above. Thus, the glass-transition-like shape of the DSC signal in Fig. 4 seems to be consistent with the Boyer and Gillham³⁸ interpretation of T_{col} and the structural changes presented in Fig. 3 for the Kirkwood factor can be also related to the suggested liquid-

liquid transition. Note that this temperature also coincides with the dynamical crossovers T_c and T_x recognized early only by dynamic methods. Thus, the heat-capacity properties near T_c and T_x could have dynamic origins. This hypothesis is also supported by the fact that the peculiarity of the DSC output at 263 K scales quite well with the heating rate (compare curves for 5 and 25 K min⁻¹ in Fig. 4).

Therefore, one can conclude that the observed changes in structure of supercooled glycerol (Fig. 3), the dynamical crossovers T_c and T_x , and unusual behavior of heat capacity (Fig. 4) tend to group near the anhydrous glycerol crystalli-

zation temperature (Figs. 1 and 2). This fact once again highlights the idea about a close relationship between the dynamics, structure, and thermodynamic properties in the supercooled liquid state which requires more experimental and theoretical investigations.

The authors express their deep gratitude to Professor A.P. Sokolov for helpful discussions as well as appreciate the creative comments of Professor R. Richert, Professor U. Kaatz, and Professor A. Schönhals and thanks to Professor J. Fontanella who drew their attention to NMR data. Y.H. is grateful to the Golda Meir Fellowship Fund for financial support.

*Also at Institute for Mechanics and Engineering of Kazan Scientific Center of Russian Academy of Science, 420111 Kazan, Russia.

†Electronic address: yurif@vms.huji.ac.il

¹C.A. Angell, *J. Non-Cryst. Solids* **131-133**, 13 (1991).

²R. Böhmer *et al.*, *J. Chem. Phys.* **99**, 4201 (1993).

³F. Stickel, E.W. Fischer, and R. Richert, *J. Chem. Phys.* **102**, 6251 (1995).

⁴F. Stickel, E.W. Fischer, and R. Richert, *J. Chem. Phys.* **104**, 2043 (1996).

⁵R. Richert and C.A. Angell, *J. Chem. Phys.* **108**, 9016 (1998).

⁶D.W. Davidson and R.H. Cole, *J. Chem. Phys.* **19**, 1484 (1951).

⁷N.O. Birge and S.R. Nagel, *Phys. Rev. Lett.* **54**, 2674 (1985).

⁸K.L. Ngai and R.W. Rendell, *Phys. Rev. B* **41**, 754 (1990).

⁹A. Schönhals *et al.*, *Phys. Rev. Lett.* **70**, 3459 (1993).

¹⁰J. Wuttke *et al.*, *Phys. Rev. Lett.* **72**, 3052 (1994).

¹¹A.P. Sokolov, W. Steffen, and E. Rössler, *Phys. Rev. E* **52**, 5105 (1995).

¹²P. Lunkenheimer *et al.*, *Phys. Rev. Lett.* **77**, 318 (1996).

¹³E. Rössler and A.P. Sokolov, *Chem. Geol.* **128**, 143 (1996).

¹⁴E. Donth *et al.*, *Thermochim. Acta* **304/305**, 239 (1997).

¹⁵T. Franosch *et al.*, *Phys. Rev. E* **55**, 3183 (1997).

¹⁶A.P. Sokolov, *J. Non-Cryst. Solids* **235-237**, 190 (1998).

¹⁷U. Schneider *et al.*, *J. Non-Cryst. Solids* **235-237**, 173 (1998).

¹⁸L. De Francesco, M. Cutroni, and A. Mandanici, *Philos. Mag. B* **82**, 625 (2002).

¹⁹P. Lunkenheimer and A. Loidl, *Chem. Phys.* **284**, 205 (2002).

²⁰A. Van Hook, *Crystallization Theory and Practice* (Reinhold, New York, 1961).

²¹H. Van Koningsveld, *Recl. Trav. Chim. Pays-Bas.* **87**, 243 (1968).

²²*Handbook of Chemistry and Physics*, edited by R.C. Weast (CRC press, Cleveland, 1974).

²³S. Havriliak and S. Negami, *J. Polym. Sci., Part C: Polym. Symp.* **14**, 99 (1966).

²⁴N. Bjerrum, *Science* **115**, 385 (1952).

²⁵D. Eiesenberg and W. Kauzmann, *The Structure and Properties of Water* (Clarendon, Oxford, 1969).

²⁶V. F. Petrenko and R. W. Whitworth, *Physics of Ice* (Oxford University Press, Oxford, 1999).

²⁷C.J.F. Böttcher and P. Bordewijk, *Theory of Electric Polarization* (Elsevier, Amsterdam, 1992).

²⁸O.A. Osipov, I.V. Minkin, and A.D. Garnovsky, *Handbook of Dipole Moments* (High School, Moscow, 1971).

²⁹W. Götze and L. Sjögren, *Rep. Prog. Phys.* **55**, 241 (1992).

³⁰F. Stickel *et al.*, *Phys. Rev. Lett.* **73**, 2936 (1994).

³¹R.F. Boyer, *J. Appl. Phys.* **25**, 825 (1954).

³²L.A. Utracki, *J. Macromol. Sci., Phys.* **B10**, 477 (1974).

³³V.P. Privalko, *Polymer* **19**, 1019 (1978).

³⁴N. Okui, *J. Mater. Sci.* **25**, 1623 (1990).

³⁵N. Okui, *Polymer* **31**, 92 (1990).

³⁶S. Umemoto and N. Okui, *Polymer* **43**, 1423 (2002).

³⁷D.E. Axelson and L. Mandelkern, *J. Polym. Sci., Polym. Phys. Ed.* **16**, 1135 (1978).

³⁸R.F. Boyer and J.K. Gillham, *J. Polym. Sci., Polym. Phys. Ed.* **19**, 13 (1981).